IEEE Access
Multidisciplinary | Rapid Review | Open Access Journal

Received July 1, 2019, accepted July 26, 2019, date of publication July 31, 2019, date of current version August 14, 2019.

Digital Object Identifier 10.1109/ACCESS.2019.2932125

Simulation and Analysis of Propagation Characteristics for Tunnel Train-Ground Communications at 1.4 and 40 GHz

TAO ZHOU[1], (Member, IEEE), HUAYU LI[1], RONGCHEN SUN[2], YANG WANG[3], LIU LIU[1], (Member, IEEE), AND CHENG TAO[1], (Member, IEEE)

[1]School of Electronics and Information Engineering, Beijing Jiaotong University, Beijing 100044, China
[2]College of Information and Communication Engineering, Harbin Engineering University, Harbin 150001, China
[3]Signal and Communication Research Institute, China Academy of Railway Sciences, Beijing 100081, China

Corresponding author: Rongchen Sun (rongchensun@hrbeu.edu.cn)

This work was supported by the Fundamental Research Funds for the Central Universities under Grant 2019JBZ001.

ABSTRACT This paper focuses on the analysis of propagation characteristics for train-ground communication (TGC) systems in tunnel scenarios at both low frequency and millimeter-wave (mmWave) bands, based on ray-tracing (RT) simulation. The material parameters in the RT simulation are calibrated by measurement data collected in realistic tunnel environments. A practical three dimension (3D) tunnel TGC environment considering the existence of train cars is established, which is further divided into three kinds of scenarios, involving the direct coverage, relay coverage, and in-train coverage scenarios. Both large-scale and small-scale propagation characteristics, such as path loss and root mean square delay spread, are analyzed for the three tunnel TGC scenarios. The obtained results can provide useful information for the design of future fifth-generation (5G) tunnel TGC systems.

INDEX TERMS 5G, train-ground communications, channel modeling, propagation characteristics, millimeter-wave, and tunnel.

I. INTRODUCTION

Train-ground communication (TGC) is the indispensable part of modern rail transit systems, e.g., railway and subway, which has always been a much-discussed research topic in both the academy and industry [1], [2]. To satisfy the increasingly higher data rate for TGC systems, fifth-generation (5G) technologies such as massive multiple-input multiple-output (MIMO) and millimeter-wave (mmWave) will be used in the TGC systems [3]. The prerequisite of designing wireless systems and evaluating transmission technologies is the understanding of propagation characteristics in operating scenarios [4], [5]. Large-scale propagation models are vital to the network deployment, which can be used to achieve the link budget and interference analysis. Small-scale fading models are essential for performance simulation and evaluation of transmission technologies. Therefore, it is quite necessary to investigate the propagation properties for 5G TGC systems.

The associate editor coordinating the review of this manuscript and approving it for publication was Cesar Briso.

The operating scenarios define the types of physical environments and relevant radio propagation mechanisms. There exist a variety of operating scenarios for TGC systems, which can be generally classified into outdoor and indoor TGC scenarios. The outdoor TGC scenarios mainly comprise viaduct, cutting, station, hilly, rural, suburban, and urban scenarios, while the indoor TGC scenarios contains tunnel and in-train scenarios. Various TGC scenarios will have different propagation characteristics.

A series of the studies have concentrated on large-scale propagation characteristics such as path loss (PL) and shadow fading in various outdoor TGC scenarios for high-speed railway (HSR), according to the narrowband channel measurements [6]–[10]. Moreover, based on the wideband multi-antenna measurement data, authors in [11]–[15] presented results of small-scale fading characteristics, including fading severity and time-frequency-space dispersion, in the HSR viaduct, cutting, station, and suburban scenarios. Besides, both large-scale and small-scale channel parameters were derived from field measurement data in hilly terrain environments on HSR [16], [17].

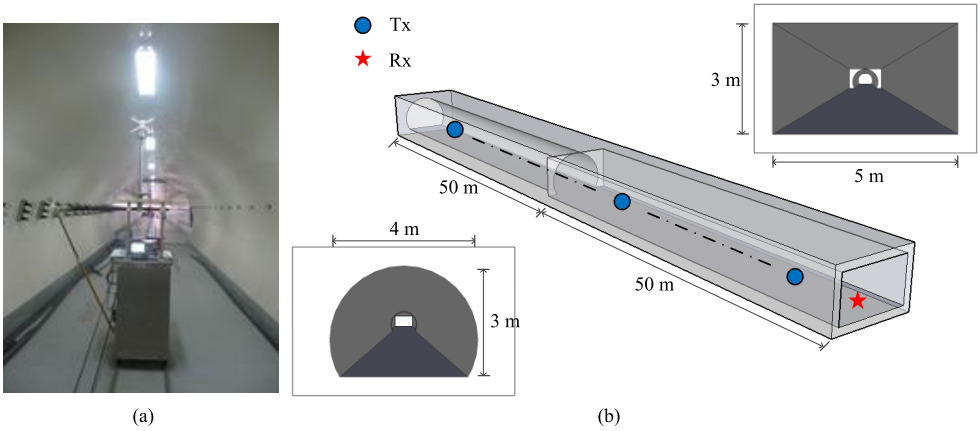

FIGURE 1. The environment and structure of the measured tunnel. (a) Measurement tunnel. (b) Geometrical structure.

However, there are relatively fewer results of propagation properties reported in the indoor TGC scenarios, especially in the tunnel scenario. This is because it is highly difficult to conduct propagation measurements for TGC in tunnel scenarios where the train cars should be included. Most of existing work focused on the propagation characteristics in tunnel without train cars. A few wideband measurements in such kind of tunnel were performed and results of PL, K-factor, and root mean square (RMS) delay spread (DS) were obtained [18]–[20]. MIMO channel measurements were conducted and both temporal and spatial characteristics were investigated in [21]–[23], which confirms the strong wave guiding effects existed in tunnel propagation. An empirical propagation model for distributed antenna systems in HSR tunnels with train cars was proposed in [24]. Due to the difficulty of tunnel measurements, some researchers employed the ray-tracing (RT) method to simulate the tunnel channel and analyze the propagation characteristics [25], [26]. However, more work should be done to calibrate the RT model using measurement data. Based on measurements conducted in a subway tunnel with train cars at 5G mmWave band, a RT model has been calibrated and used to analyze more mmWave propagation characteristics [27]. In the RT simulation only direct coverage mode is considered, in which the receive antenna is installed on the middle of the front window inside train cars, whereas the relay coverage mode with the receive antenna placed on top of the train is ignored.

To fill the aforementioned research gaps, this paper presents the RT simulation and propagation analysis for TGC in tunnel scenarios with train cars at both low frequency and mmWave bands. Firstly, the material parameters considered in the simulation are calibrated by measurement results in an experimental tunnel. Then, by expanding the geometrical size of the experimental tunnel and using the calibrated material parameters, three TGC scenarios, such as direct coverage, relay coverage, and in-train coverage scenarios, are simulated. Finally, propagation characteristics, including PL and RMS DS, are obtained and analyzed for the three TGC tunnel scenarios.

The remainder of this paper is outlined as follows. Section II describes measurement campaigns and ray tracer calibration. In Section III, the scenarios and configuration in the RT simulation is introduced. Simulation results and analysis are presented in Section IV. Finally, conclusions are drawn in Section V.

II. MEASUREMENTS AND CALIBRATION

A. MEASUREMENT CAMPAIGNS

The measurements were conducted in an experimental tunnel with relatively smaller size, built by Zhongtian Technology Group Company in China [28]. The environment and structure of the measured tunnel are illustrated in Fig. 1. To match the realistic underground tunnel environment, the tunnel wall was made by reinforced concrete. The entire tunnel with 3 m height has a composite structure that is divided into two equal segments with 50 m length for each. The shape of cross section in one segment is rectangle, while another is horseshoe. The interior widths of the rectangle and horseshoe parts are 5 m and 4 m, respectively.

The employed channel sounder is composed of a vector signal generator, as the transmitter (Tx), and a customized data collector, as the receiver (Rx). The synchronization signal is transmitted by an optical fiber to both Tx and Rx. The Rx is used to collect the transmitted Zadoff-Chu (ZC) sequence and to obtain the channel impulse responses (CIRs) by sliding correlation of the collected data and the local ZC sequence copy. The Rx keeps static at the end of tunnel in the rectangular segment, while the Tx moves to the other side. The vertically polarized omnidirectional antennas are equipped at both Tx and Rx sides and the height is 2.5 m. The measurement frequency is set to 1.4 GHz. During the range of 100 m, the CIRs are collected by interval of 1 m.

B. RAY TRACER CALIBRATION

Based on the acquired measurement data, the material parameters of tunnel configured in ray tracer can be calibrated. The RT tool employed in the paper is Wireless InSite [29]. By reconstructing the three dimension (3D)

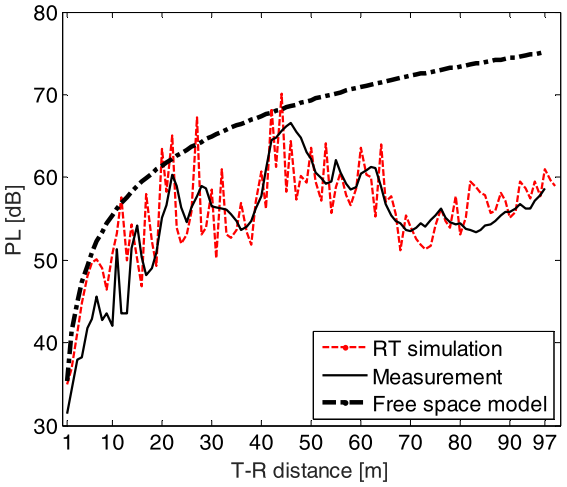

FIGURE 2. Comparison of PL results in the measurement and RT simulation.

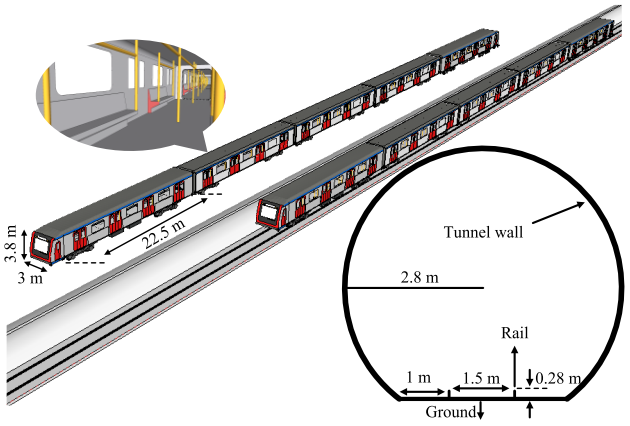

FIGURE 3. The established 3D tunnel environment with train cars in RT simulation.

TABLE 1. Antenna configuration for the three scenarios.

Scenario	Frequency (GHz)	Radiation	Polarization
Direct coverage	1.4	Omnidirectional	Vertical
Relay coverage	1.4/40	Omnidirectional	Vertical
In-train coverage	40	Omnidirectional	Vertical, Horizontal

tunnel environment and setting the material parameters, simulation results for propagation characteristics can be obtained. The material parameters will be adjusted to achieve an appropriate agreement between the simulated and measured results. Fig. 2 compares the PL results in the measurement and RT simulation. The antenna parameters such as frequency and antenna type are the same as those in the measurement. The material parameters of tunnel wall are configured as follows: relative permittivity is 5.31, conductivity is 0.0428 S/m, thickness is 0.3 m, and roughness is 0.002. According to the comparison, it is observed that the PL results in the measurement and RT simulation accomplish an acceptable match. This confirms that the used material parameters in the ray tracer are able to approximate realistic values. The calibrated material parameters will be used in further RT simulation, where the 3D tunnel environments with different geometrical sizes are employed.

III. RAY-TRACING BASED SIMULATION

A. SCENARIO DESCRIPTION

The tunnels used for rail transit systems commonly have larger structure than the tested one. Moreover, tunnel TGC should consider the existence of train cars. Therefore, to obtain reliable propagation characteristics in such scenarios, a more practical 3D tunnel TGC environment is established, as shown in Fig. 3. The tunnel has a horseshoe shaped cross section with the larger geometrical size, which is established according to the specification of subway tunnels. The material of tunnel is concrete, the same as the measured one. In addition, five train cars with each of 22.5 m length, 3 m width, 3.8 m height, 4 pairs of door, and 3 pairs of window are added into the tunnel. There are several long chairs and vertical handrails inside the train cars, while passengers are not included in the model.

As for tunnel TGC, two typical coverage modes are considered in the paper, including direct coverage and relay coverage modes. The direct coverage mode means that the communication link is from base station on the ground to the passengers inside the train cars. This communication mode suffers from the severe penetration loss yielded by the train cars. Thus, the high frequency band is not suitable in this case. The relay coverage mode means that one communication link is from base station to relay station on top of the train cars, another communication link is from relay station to passengers. This mode can effectively avoid the penetration loss and is appropriate for both high and low frequency bands. The two coverage modes correspond to three propagation scenarios, involving direct coverage, relay coverage, and in-train coverage scenarios. This paper will investigate the propagation properties in the three scenarios, respectively.

B. SIMULATION CONFIGURATION

With regard to the three scenarios, the RT simulation is configured differently. The antenna parameters are listed in Table 1. The frequency is set to 1.4 GHz for the direct coverage scenario, 1.4 and 40 GHz for the relay coverage scenario, and 40 GHz for the in-train coverage scenario. The antenna radiation is omnidirectional for both frequencies. The in-train coverage case considers different polarization modes, including horizontal and vertical polarization, while the other two scenarios only use the vertical polarization.

The position distributions of Tx and Rx antennas for the three scenarios in the RT simulation are illustrated in Fig. 4. As for the direct coverage scenario shown in Fig. 4(a), the Tx antenna is placed at the center of tunnel and has the 2.7 m height, while the Rx antenna with the height of 2.2 m is located from the Tx antenna at 1 m interval until to the distance of 100 m. It is noted that the Rx antenna is located inside the train cars from 60 to 100 m. With regard to the relay

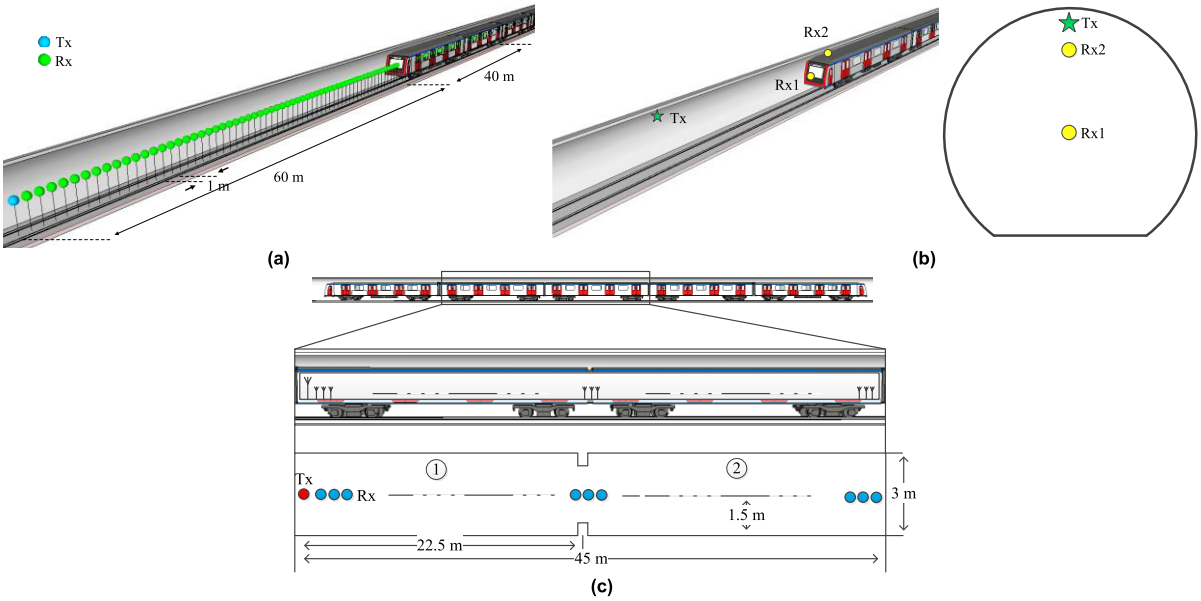

FIGURE 4. The position distributions of Tx and Rx antennas in RT simulation. (a) Direct coverage scenario. (b) Relay coverage scenario. (c) In-train coverage scenario.

TABLE 2. Configuration of material parameters for the three scenarios.

Item	Material	Frequency (GHz)	Relative permittivity	Conductivity (S/m)	Thickness (m)	Roughness
Tunnel wall	Concrete	1.4 40	5.31	0.0428 0.6458	0.30	0.002
Train window	Glass	1.4 40	6.27	0.007 0.3499	0.01	0
Train car	Metal	-	1	10^7	-	-

coverage scenario shown in Fig. 4(b), the Tx antenna is put on top of tunnel, and two cases of the Rx antenna position are considered. Rx1 is placed at the front of train cars and close to the front window, with the height of 2.2 m, while Rx2 is put on the top of train cars and has the 1 m distance away from the front of train cars. In the in-train coverage scenario, as shown in Fig. 4(c), the Tx antenna is located in the center of the first train car and has the height of 2 m, while the Rx antenna with the 1.5 m height is placed away from Tx at 0.2 m interval until to end of the second train car.

In the RT simulation, three kinds of material are considered, including concrete, glass, and metal. Table 2 lists the configuration of material parameters. The setting of electromagnetic parameters for concrete at 1.4 GHz uses the calibrated results as mentioned in Section II.C, whereas the configuration for material parameters at the high frequency band employs the values recommended in ITU-R P.2040 [30]. Besides, the number of reflections is set to 8, and assuming that no more than 100 rays can be received.

IV. RESULTS AND ANALYSIS

A. DIRECT COVERAGE SCENARIO

As for the direct coverage scenario, the PL results for cases with and without train cars are presented, and compared with the free space model, as shown in Fig. 5. It is found that the PL values for cases with and without train cars are similar when the distance between Tx and Rx antennas (T-R distance) is less than 60 m. This means that in the tunnel the train cars have almost no influence on the PL when the Rx antenna is placed outside and away from the train cars. However, the values for the case with train cars significantly increase

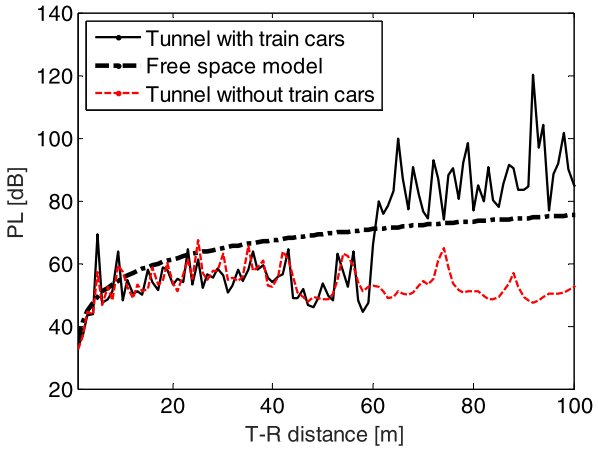

FIGURE 5. PL results for different cases in the direct coverage scenario.

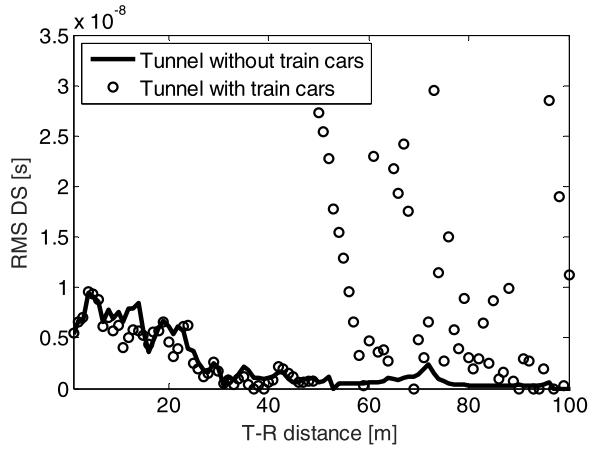

FIGURE 6. RMS DS results for different cases in the direct coverage scenario.

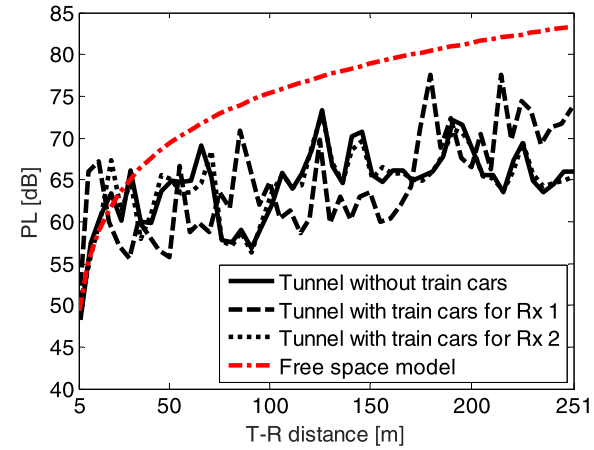

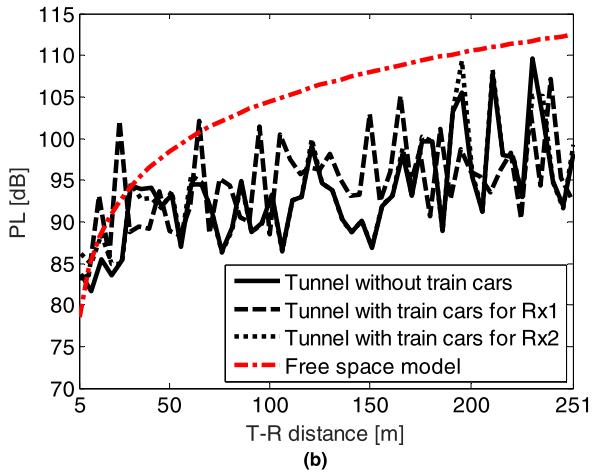

FIGURE 7. PL results for different cases in the relay coverage scenario. (a) 1.4 GHz. (b) 40 GHz.

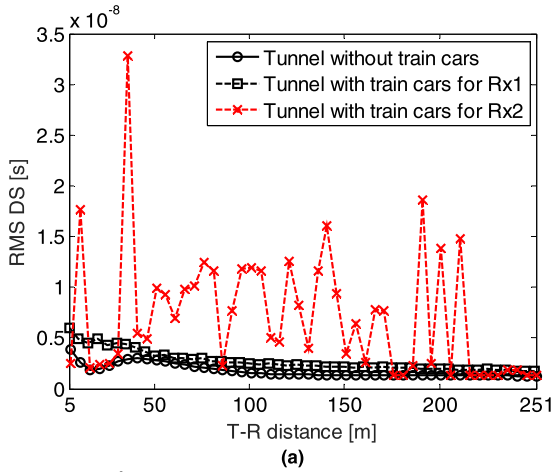

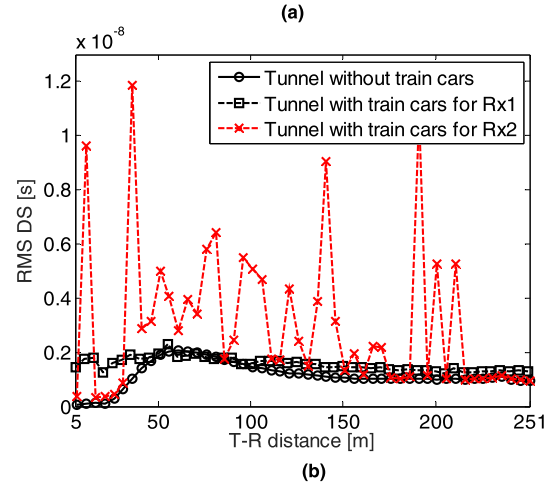

FIGURE 8. RMS DS results for different cases in the relay coverage scenario. (a) 1.4 GHz. (b) 40 GHz.

TABLE 3. Statistical results of RMS DS for different cases in the relay coverage scenario.

Frequency (GHz)	Rx position	Train cars	RMS DS (ns) Mean value	Standard deviation	Maximum value
1.4	Rx1	Without	2.26	0.79	4.88
		with	2.71	0.99	6.01
	Rx2	Without	1.75	0.62	3.86
		with	7.14	6.13	32.86
40	Rx1	Without	1.17	0.33	1.45
		with	1.56	0.24	2.29
	Rx2	Without	1.16	0.48	2.05
		with	3.05	2.72	11.88

and fluctuate more dramatic when the T-R distance exceeds 60 m, which are much higher than the results of the free space model. This is because as the T-R distance is over 60 m, the Rx antenna is inside the train cars and suffers from the penetration loss. According to the comparison between the values for the cases with and without train cars, it is estimated that the penetration loss of train cars will be around 30 dB. This is in accordance with some measurement results [31].

Fig. 6 shows the RMS DS results for cases with and without train cars in the direct coverage scenario. It can be seen that when the T-R distance is less than 50 m, the RMS DS gradually decreases with distance for both cases. This is due to the special propagation environment in tunnel where the propagation distance between multipath components (MPCs) is shortening as the T-R distance increases, leading to the

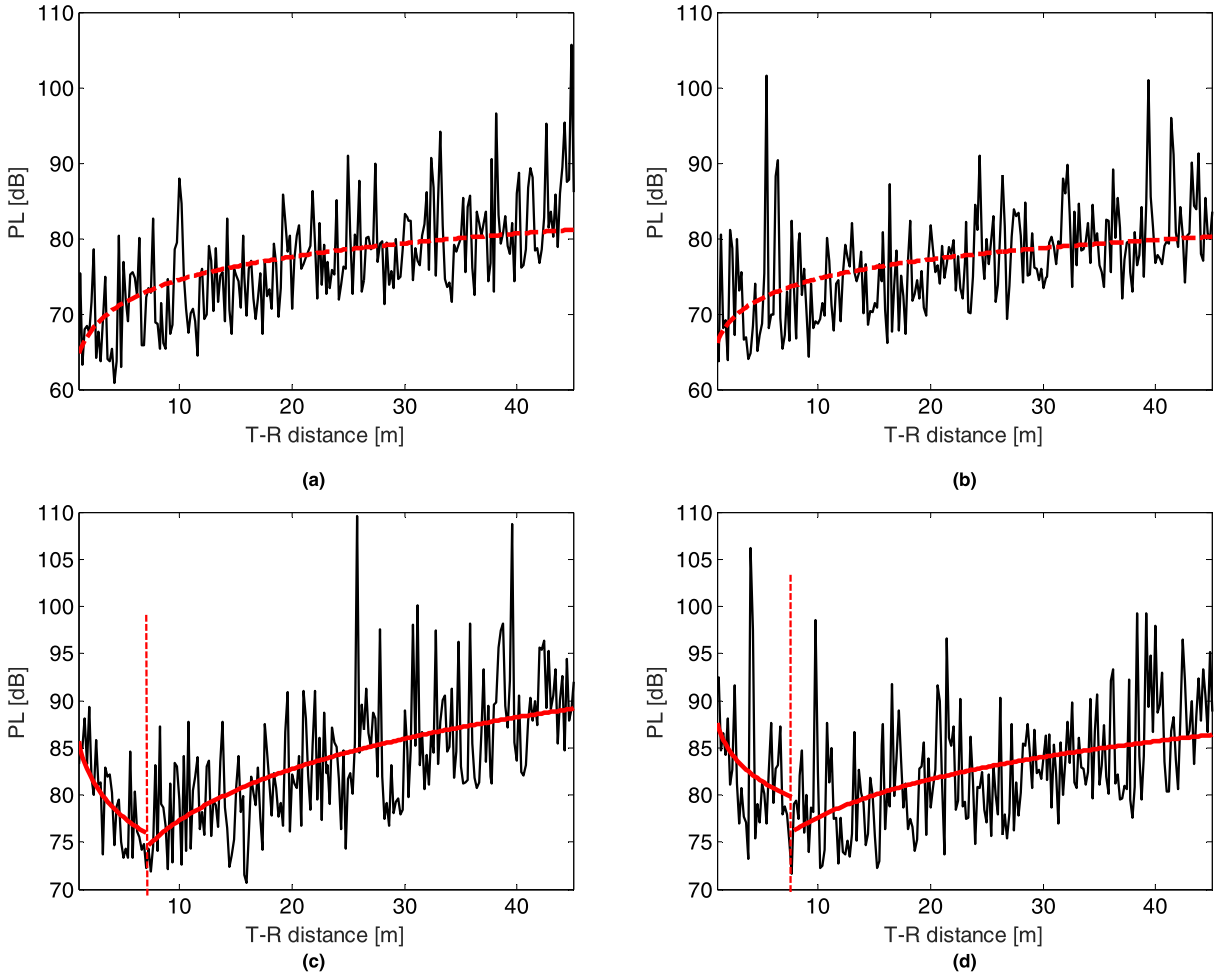

FIGURE 9. PL results for different polarization modes in the in-train coverage scenario. (a) V-V. (b) H-H. (c) V-H. (d) H-V.

reduced time delay difference between MPCs. It can be also found that when the T-R distance is over 50 m, the RMS DS for the case with train cars begins to increase dramatically. This is reasonable that more reflecting MPCs caused by the train cars appear when the Rx antenna is 10 m away from the train cars or when the Rx antenna is inside the train cars. In this case, the maximum RMS DS can reach almost 30 ns.

TABLE 4. Fitting results of PL for different polarization modes in the in-train coverage scenario.

Polarization mode	BP	Intercept value	PL exponent
V-V	-	64.34	1.017
H-H	-	66.13	0.8531
V-H	Before	85.76	-1.161
	After	59.1	1.818
H-V	Before	87.7	-0.8948
	After	64.24	1.339

B. RELAY COVERAGE SCENARIO

The PL results for cases of Rx1 and Rx2 in the relay coverage scenario at 1.4 and 40 GHz are provided and the cases with and without train cars are also compared, as illustrated in Fig. 7. It is observed that there is less impact of the train cars and Rx antenna position on the PL variation for both 1.4 and 40 GHz frequencies. In addition, the PL values at 40 GHz are about 30 dB higher than that at 1.4 GHz, which is in accordance with the results of free space model.

Fig. 8 compares the RMS DS results for the cases of Rx1 and Rx2 and the cases with and without train cars in the relay coverage scenario at 1.4 and 40 GHz. It can be seen that the existence of train cars has an obvious influence on the RMS DS for the case of Rx2 at 1.4 and 40 GHz, whereas it slightly affects the result for the case of Rx1. This is because when the Rx antenna is placed on top of train cars, it can receive extra MPCs produced by the train cars, such as the roof and both sides of train cars. However, if the Rx antenna is quite close to the front of train cars, it will be impossible to receive reflecting waves caused by the train cars. In this case, the RMS DS for Rx2 is much worse than that for Rx1. It can be also observed that the impact of train cars is weakening when the T-R distance exceeds 200 m.

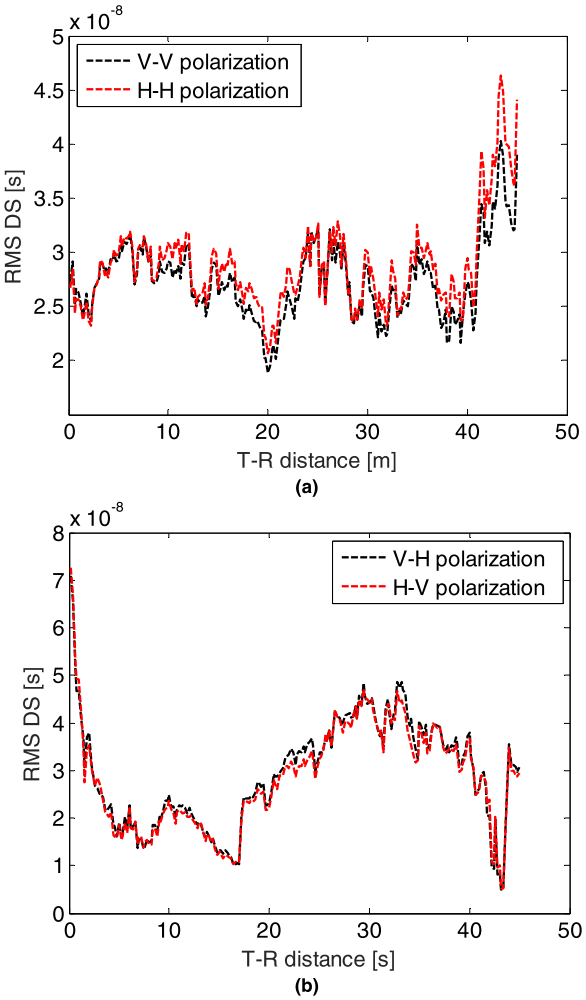

FIGURE 10. RMS DS results for different polarization modes in the in-train coverage scenario. (a) Co-polarization. (b) Cross-polarization.

Table 3 lists the statistical results of RMS DS for the different cases at 1.4 and 40 GHz. It is found that when the Rx antenna is located at Rx1, the mean value of RMS DS for the case with train cars is almost 3 times higher than that for the case without train cars. In addition, the statistical values of RMS DS at 40 GHz are much lower than those at 1.4 GHz. This is due to the higher attenuation of MPCs at high frequency band.

C. IN-TRAIN COVERAGE SCENARIO

With regard to the in-train coverage scenario, four kinds of combination for Tx and Rx polarization modes are considered, e.g., vertical-vertical (V-V), horizontal-horizontal (H-H), vertical-horizontal (V-H), and horizontal-vertical (H-V). Fig. 9 illustrates the PL results and corresponding fitting curves using the well-known log-distance PL model for the four types. It is obvious that the PL for the cross-polarization (V-V or H-H) is higher than the co-polarization (V-H or H-V). As for the co-polarization mode, the PL curves appear a break point (BP) at round 7 m.

TABLE 5. Statistical results of RMS DS for different polarization modes in the in-train coverage scenario.

Polarization mode	BP	RMS DS (ns) Mean value	Standard deviation	Maximum value
V-V	-	27.31	3.54	40.29
H-H	-	28.72	4.18	46.32
V-H	Before	28.31	13.95	70.84
	After	29.37	10.62	48.53
H-V	Before	27.04	14.47	72.62
	After	28.69	10.17	47.13

The PL decreases with the T-R distance before BP, whereas it increases after BP. In addition, the 40 GHz PL results with co-polarization in the in-train coverage scenario are almost 15 dB lower than the values in the relay coverage scenario. The fitting results of PL for the four types of polarization modes are listed in Table 4. The difference of the PL values between the co-polarization and cross-polarization is around 10 dB. The cross-polarization has the larger PL exponent than the co-polarization.

The results of RMS DS for the four types of polarization modes are shown in Fig. 10. It can be found that before BP, the RMS DS decreases dramatically. Table 5 lists the statistical parameters of RMS DS for different polarization modes. It is observed that the mean value of RMS DS for the four modes is similar, whereas the standard deviation of RMS DS for the cross-polarization is higher than that for the co-polarization. In addition, the 40 GHz RMS DS results in the in-train coverage scenario are much larger than the values in the relay coverage scenario.

V. CONCLUSION

In this paper, we have investigated propagation characteristics for tunnel TGC scenarios at 1.4 and 40 GHz, according to the RT simulation. Realistic channel measurement data are collected in the experimental tunnel and used for calibrating the material parameters. Three kinds of 3D tunnel TGC scenarios, such as the direct coverage, relay coverage, and in-train coverage scenarios are established. The PL and RMS DS results are obtained and analyzed for the three scenarios. It is shown that the train cars introduce more MPCs for the direct coverage scenario, and have stronger impact on the RMS DS than the PL for the relay coverage scenario. It is also seen that the propagation characteristics are quite different for co-polarization and cross-polarization modes in the in-train coverage scenario. These results will provide a reference for the design of tunnel 5G TGC systems.

REFERENCES

[1] B. Ai, X. Cheng, T. Kürner, Z.-D. Zhong, K. Guan, R.-S. He, L. Xiong, D. W. Matolak, D. G. Michelson, and C. B. Rodriguez, "Challenges toward wireless communications for high-speed railway," *IEEE Trans. Intell. Transp. Syst.*, vol. 15, no. 5, pp. 2143–2158, Oct. 2014.

[2] R. He, B. Ai, G. Wang, K. Guan, Z. Zhong, A. F. Molisch, C. Briso-Rodriguez, and C. P. Oestges, "High-speed railway communications: From GSM-R to LTE-R," *IEEE Veh. Technol. Mag.*, vol. 11, no. 3, pp. 49–58, Sep. 2016.

[3] B. Ai, K. Guan, M. Rupp, T. Kurner, X. Cheng, X.-F. Yin, Q. Wang, G.-Y. Ma, Y. Li, L. Xiong, and J.-W. Ding, "Future railway services-oriented mobile communications network," *IEEE Commun. Mag.*, vol. 53, no. 10, pp. 78–85, Oct. 2015.
[4] T. Zhou, H. Li, Y. Wang, L. Liu, and C. Tao, "Channel modeling for future high-speed railway communication systems: A survey," *IEEE Access*, vol. 7, no. 1, pp. 52818–52826, Apr. 2019.
[5] T. Zhou, C. Tao, S. Salous, L. Liu, and Z. Tan, "Channel sounding for high-speed railway communication systems," *IEEE Commun. Mag.*, vol. 53, no. 10, pp. 70–77, Oct. 2015.
[6] R. He, Z. Zhong, B. Ai, and J. Ding, "An empirical path loss model and fading analysis for high-speed railway viaduct scenarios," *IEEE Antennas Wireless Propag. Lett.*, vol. 10, pp. 808–812, Aug. 2011.
[7] R. He, Z. Zhong, B. Ai, and J. Ding, "Propagation measurements and analysis for high-speed railway cutting scenario," *Electron. Lett.*, vol. 47, no. 21, pp. 1167–1168, Oct. 2011.
[8] K. Guan, Z. Zhong, B. Ai, and T. Kürner, "Empirical models for extra propagation loss of train stations on high-speed railway," *IEEE Trans. Antennas Propag.*, vol. 62, no. 3, pp. 1395–1408, Mar. 2014.
[9] K. Guan, Z. Zhong, B. Ai, and T. KÃijürner, "Propagation measurements and analysis for train stations of high-speed railway at 930 MHz," *IEEE Trans. Veh. Technol.*, vol. 63, no. 8, pp. 3349–3516, Oct. 2014.
[10] R. He, Z. Zhong, B. Ai, G. Wang, J. Ding, and A. F. Molisch, "Measurements and analysis of propagation channels in high-speed railway viaducts," *IEEE Trans. Wireless Commun.*, vol. 12, no. 2, pp. 794–805, Feb. 2013.
[11] T. Zhou, C. Tao, S. Salous, L. Liu, and Z. Tan, "Channel characterization in high-speed railway station environments at 1.89 GHz," *Radio Sci.*, vol. 50, no. 11, pp. 1176–1186, Dec. 2015.
[12] T. Zhou, C. Tao, S. Salous, and L. Liu, "Measurements and analysis of angular characteristics and spatial correlation for high-speed railway channels," *IEEE Trans. Intell. Transp. Syst.*, vol. 19, no. 2, pp. 357–367, Feb. 2018.
[13] T. Zhou, C. Tao, S. Salous, and L. Liu, "Measurements and analysis of short-term fading behavior in high-speed railway communication networks," *IEEE Trans. Veh. Technol.*, vol. 68, no. 1, pp. 101–112, Jan. 2019.
[14] T. Zhou, C. Tao, and L. Liu, "LTE-assisted multi-link MIMO channel characterization for high-speed train communication systems," *IEEE Trans. Veh. Technol.*, vol. 68, no. 3, pp. 2044–2051, Mar. 2019.
[15] T. Zhou, C. Tao, S. Salous, and L. Liu, "Joint channel characteristics in high-speed railway multi-link propagation scenarios: Measurement, analysis, and modeling," *IEEE Trans. Intell. Transp. Syst.*, vol. 20, no. 6, pp. 2367–2377, Jun. 2019. doi: 10.1109/TITS.2018.2868973.
[16] F. Luan, Y. Zhang, L. Xiao, C. Zhou, and S. Zhou, "Fading characteristics of wireless channel on high-speed railway in hilly terrain scenario," *Int. J. Antennas Propag.*, vol. 2013, Jan. 2013, Art. no. 378407.
[17] Y. Zhang, Z. He, W. Zhang, L. Xiao, and S. Zhou, "Measurement-based delay and Doppler characterizations for high-speed railway hilly scenario," *Int. J. Antennas Propag.*, vol. 2014, Apr. 2014, Art. no. 875345.
[18] P. Aikio, R. Gruber, and P. Vainikainen, "Wideband radio channel measurements for train tunnels," in *Proc. 48th IEEE Veh. Technol. Conf. (VTC)*, May 1998, pp. 460–464.
[19] J.-M. Molina-Garcia-Pardo, M. Lienard, A. Nasr, and P. Degauque, "Wideband analysis of large scale and small scale fading in tunnels," in *Proc. 8th Int. Conf. Intell. Transp. Syst. Telecommun. (ITST)*, Phuket, Thailand, Oct. 2008, pp. 270–273.
[20] L. Zhang, C. Briso, J. R. O. Fernandez, J. I. Alonso, C. Rodríguez, J. M. García-Loygorri, and K. Guan, "Delay spread and electromagnetic reverberation in subway tunnels and stations," *IEEE Antennas Wireless Propag. Lett.*, vol. 15, pp. 585–588, 2016.
[21] M. Lienard, P. Degauque, J. Baudet, and D. Degardin, "Investigation on MIMO channels in subway tunnels," *IEEE J. Sel. Areas Commun.*, vol. 21, no. 3, pp. 332–339, Apr. 2003.
[22] J. A. Valdesueiro, B. Izquierdo, and J. Romeu, "On 2 × 2 MIMO observable capacity in subway tunnels at *C*-band: An experimental approach," *IEEE Antennas Wireless Propag. Lett.*, vol. 9, pp. 1099–1102, 2010.
[23] E. Masson, Y. Cocheril, M. Berbineau, J.-P. Ghys, V. Hovinen, and A. Roivainen, "MIMO channel characterization in subway tunnel for train-to-wayside applications," in *Proc. 12th Int. Conf. ITS Telecommun. (ITST)*, Taipei, Taiwan, Nov. 2012, pp. 732–736.
[24] C. Briso-Rodriguez, J. M. Cruz, and J. I. Alonso, "Measurements and modeling of distributed antenna systems in railway tunnels," *IEEE Trans. Veh. Technol.*, vol. 56, no. 5, pp. 2870–2879, Sep. 2007.
[25] C. Gentile, F. Valoit, and N. Moayeri, "A raytracing model for wireless propagation in tunnels with varying cross section," in *Proc. IEEE Global Commun. Conf. (GLOBECOM)*, Anaheim, CA, USA, Dec. 2012, pp. 5027–5032.
[26] N. Sood, L. Liang, S. V. Hum, and C. D. Sarris, "Ray-tracing based modeling of ultra-wideband pulse propagation in railway tunnels," in *Proc. IEEE Int. Symp. Antennas Propag. (APSURSI)*, Spokane, WA, USA, Jul. 2011, pp. 2383–2386.
[27] D. He, B. Ai, K. Guan, Z. Zhong, B. Hui, J. Kim, H. Chung, and I. Kim, "Channel measurement, simulation, and analysis for high-speed railway communications in 5G millimeter-wave band," *IEEE Trans. Intell. Transp. Syst.*, vol. 19, no. 10, pp. 3144–3158, Oct. 2018.
[28] R. Sun, D. W. Matolak, C. Tao, L. Liu, Z. Tan, and T. Zhou, "Investigation of MIMO channel characteristics in a two-section tunnel at 1.4725 GHz," *Int. J. Antennas Propag.*, vol. 2017, Jul. 2017, Art. no. 3693149.
[29] *Wireless InSite 3D Wireless Prediction Software*. Accessed: May 20, 2019. [Online]. Available: https://www.remcom.com/wireless-insite-em-propagation-software
[30] *Effects of Building Materials and Structures on Radiowave Propagation Above About 100 MHz*, document ITU-R P. 2040, Jul. 2015.
[31] T. Zhou, C. Tao, S. Salous, L. Liu, and Z. Tan, "Implementation of an LTE-based channel measurement method for high-speed railway scenarios," *IEEE Trans. Instrum. Meas.*, vol. 65, no. 1, pp. 25–36, Jan. 2016.

TAO ZHOU (M'16) received the B.E. degree from the Changchun University of Science and Technology, Changchun, China, in 2009, and the Ph.D. degree from Beijing Jiaotong University, Beijing, China, in 2016. From 2014 to 2015, he was a visiting Ph.D. Student with the Centre for Communication Systems, School of Engineering and Computing Sciences, Durham University, U.K. Since 2016, he has an Associate Professor with the School of Electronics and Information Engineering, Beijing Jiaotong University. His current research interests include channel sounding and modeling, high-speed railway communications, machine learning, and deep learning in communications.

HUAYU LI received the B.E. degree from Beijing Jiaotong University (BJTU), Beijing, China, in 2018, where she is currently pursuing the master's degree in communication and information systems. Her current research interests include propagation channel characterization and channel modeling for high-speed railway communication systems.

RONGCHEN SUN received the B.E. and Ph.D. degrees from Beijing Jiaotong University (BJTU), Beijing, China, in 2010 and 2018, respectively. From 2015 to 2016, he was a visiting Ph.D. Student with the School of Electric Engineering, University of South Carolina, USA. Since 2018, he has been an Associate Professor with the College of Information and Communication Engineering, Harbin Engineering University. His current research interests include propagation channel characterization, channel sounding and modeling for high-speed railway, and subway tunnel communication systems.

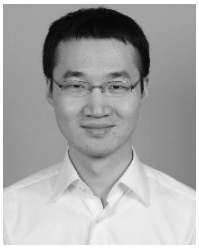

YANG WANG received the B.E. degree from Yan'an University, Shanxi, China, in 2009, and the master's degree from Beijing Jiaotong University, Beijing, China, in 2012. From 2013 to 2018, he was with the Institute of Computing Technology, China Academy of Railway Sciences. Since 2018, he has been with the Signal and Communication Research Institute, China Academy of Railway Sciences. His current research interests include the GSM-R synchronous operation and the control system of locomotives, LTE-R field strength test, and the research of railway next generation mobile communication systems.

LIU LIU (M'12) received the B.E. and Ph.D. degrees from Beijing Jiaotong University (BJTU), Beijing, China, in 2004 and 2010, respectively. He was a post Ph.D. Researcher with the School of Electronics and Information Engineering, Institute of Broadband Wireless Mobile Communications, BJTU, from 2010 to 2012, where he has been a Full Professor, since 2018. His current research interests include channel measurement and modeling for different propagation environments and signal processing of wireless communication in time-varying channel.

CHENG TAO (M'95) received the M.S. degree from Xidian University, Xian, China, in 1989, and the Ph.D. degree from Southeast University, Nanjing, China, in 1992, both in telecommunication and electronic system. He was a Postdoctoral Fellow of the School of Electronics and Information Engineering, Beijing Jiaotong University (BJTU), Beijing, China, from 1993 to 1995. From 1995 to 2006, he was with the Air Force Missile College and the Air Force Commander College. In 2006, he joined as an Academic Faculty Member of BJTU, where he is currently a Full Professor and the Director of the Institute of Broadband Wireless Mobile Communications. He has authored over 50 papers. He holds 20 patents. His current research interests include mobile communications, multiuser signal detection, radio channel measurement and modeling, and signal processing for communications.